

## Band anticrossing in highly mismatched $\text{Sn}_x\text{Ge}_{1-x}$ semiconducting alloys

K. Alberi,<sup>1,2</sup> J. Blacksberg,<sup>3</sup> L. D. Bell,<sup>3</sup> S. Nikzad,<sup>3</sup> K. M. Yu,<sup>1</sup> O. D. Dubon,<sup>1,2</sup> and W. Walukiewicz<sup>1</sup>

<sup>1</sup>Materials Sciences Division, Lawrence Berkeley National Laboratory, Berkeley, California 94720, USA

<sup>2</sup>Department of Materials Science and Engineering, University of California, Berkeley, California 94720, USA

<sup>3</sup>Jet Propulsion Laboratory, California Institute of Technology, Pasadena, California 91109, USA

(Received 13 August 2007; revised manuscript received 1 November 2007; published 8 February 2008)

We show that at dilute Sn concentrations ( $x < 10\%$ ), the composition dependence of the direct band gap and spin-orbit splitting energies of  $\text{Sn}_x\text{Ge}_{1-x}$  can be described by a valence band anticrossing model. Hybridization of the extended and localized  $p$ -like states of the Ge host matrix and the Sn minority atoms, respectively, leads to a restructuring of the valence band into  $E_+$  and  $E_-$  subbands. The notably large reduction in the band gap follows from an upward shift in the valence band edge by approximately 22 meV per  $x=0.01$ . These results demonstrate that like III-V and II-VI compound semiconductors, group IV elements may form highly mismatched alloys in which the band anticrossing phenomenon is responsible for their unique properties.

DOI: [10.1103/PhysRevB.77.073202](https://doi.org/10.1103/PhysRevB.77.073202)

PACS number(s): 78.66.Li, 71.22.+i, 78.20.Ek

For over a decade,  $\text{Sn}_x\text{Ge}_{1-x}$  has been touted as the first direct band gap semiconductor composed entirely of group IV elements.<sup>1-4</sup> The addition of  $\alpha$ -Sn, a zero-gap semiconductor, to Ge has been shown to significantly reduce both the indirect and direct band gap energies, with a crossover to a direct gap occurring in the alloy at compositions around  $x=0.1$ .<sup>2,3</sup> A recent theoretical investigation also suggests that in the dilute limit, strained  $\text{Sn}_x\text{Ge}_{1-x}$  may exhibit enhanced electron and hole mobilities compared to Ge.<sup>5</sup> The tunable nature of this low-energy direct gap certainly makes  $\text{Sn}_x\text{Ge}_{1-x}$  a compelling material for infrared applications, and if the high mobility predictions hold true, this alloy could be attractive for high speed integrated circuits as well.

Despite the progress in current research on  $\text{Sn}_x\text{Ge}_{1-x}$ , uncertainties remain regarding the fundamental basis of the alloy's optical and electrical properties, which is ultimately rooted in the composition dependence of its band structure. In particular, the large bowing of the direct band gap as well as the indirect to direct gap crossover at such a low Sn concentration are remarkable and require further investigation. The composition dependence of an alloy's band gap can be estimated to a first degree by the linear interpolation between the values of the endpoint materials,  $A$  and  $B$ , assumed by the virtual crystal approximation (VCA). However, semiconductor alloys usually exhibit some deviation, or bowing, away from this trend due primarily to constituent mismatch and disorder related potential fluctuations. Instead, the bowing is typically described by a quadratic relationship between the two gaps using an empirically determined bowing parameter  $b$  to characterize the degree of divergence from the VCA,

$$E_g^{\text{alloy}}(x) = E_g^A x + E_g^B (1-x) - bx(1-x).$$

The bowing in the individual conduction and valence bands is then generally determined by the relative band offsets of the endpoint components, given as

$$b_{\text{band edge}} = \left( \frac{\Delta E_{\text{band edge}}}{\Delta E_g} \right) b.$$

Previous investigations have established a bowing parameter  $b=1.94$  eV for the direct gap of  $\text{Sn}_x\text{Ge}_{1-x}$ ,<sup>3</sup> and assuming a

type I band alignment between Ge and  $\alpha$ -Sn with conduction and valence band offsets of  $-1.0$  and  $0.2$  eV, respectively, the majority of this bowing is expected to occur at the conduction band edge ( $b_{CB}=1.62$  eV) rather than in the valence band ( $b_{VB}=0.32$  eV).<sup>6</sup> While the values of  $b$  required to satisfy the bowing in most alloys are typically smaller than their band gaps, such as in the case of  $\text{Si}_x\text{Ge}_{1-x}$  ( $b=0.14$ ), the bowing parameter determined for  $\text{Sn}_x\text{Ge}_{1-x}$  is more than twice the direct gap of Ge, suggesting that other interactions have a noticeable effect on the band structure of the alloy.<sup>3</sup> Furthermore, the composition at which the indirect to direct gap transition takes place does not correspond to those predicted by the VCA (at  $x=0.26$ ) or the quadratic bowing relationship (at  $x=0.06$ ). These inconsistencies necessitate a more rigorous approach for understanding the origin of the optical properties of this alloy.

In this Brief Report, we show that the optical properties of  $\text{Sn}_x\text{Ge}_{1-x}$  may be accurately explained through the application of a valence band anticrossing (VBAC) model. A restructuring of the valence band occurs via an anticrossing interaction between the extended  $p$ -like states of the Ge matrix and the localized  $p$ -like states of the metallic Sn impurities, leading to a rather significant bowing of the valence band edge in contrast to that of the conduction band. This model provides the physical underpinnings to the band gap bowing in  $\text{Sn}_x\text{Ge}_{1-x}$  and, more generally, describes the ubiquitous nature of the band anticrossing phenomenon in group IV-IV highly mismatched alloys (HMAs).

It has been known for some time that III-V and II-VI compounds exhibit similarly large band gap bowing when the anion sublattice is partially replaced by an isoelectronic element of much different electronegativity or ionization energy. The properties and electronic structure of these HMAs, including  $\text{GaN}_x\text{As}_{1-x}$ ,  $\text{GaBi}_x\text{As}_{1-x}$ ,  $\text{ZnO}_x\text{Te}_{1-x}$ , and  $\text{ZnTe}_x\text{S}_{1-x}$ , have since been understood in terms of a band anticrossing (BAC) model.<sup>7-10</sup> Highly electronegative, isoelectronic minority atoms, such as N in GaAs or O in ZnTe, introduce localized  $s$ -like states near the conduction band edge of the host compound, while large metallic minority atoms with a much lower ionization energy than that of the host anion, i.e., As in GaN or Te in ZnO, introduce localized

$p$ -like states near the valence band edge. The BAC model predicts that an anticrossing interaction between the localized states of these minority atoms and the extended states of the host leads to a restructuring of the conduction or valence band into  $E_+$  and  $E_-$  subbands, when the minority species is much more electronegative or has a much lower ionization energy than the host, respectively. As a result, there is a significant change in the dispersion relation as well as a shift in the band edge position that enhances the band gap bowing and influences the optical and electrical properties of the alloy. For example, bowing in the conduction band edge is responsible for the large band gap bowing observed in  $\text{GaN}_x\text{As}_{1-x}$ , while bowing in the valence band edge is the source of the band gap bowing in  $\text{GaBi}_x\text{As}_{1-x}$ .<sup>7,8</sup> It follows from this previous work on compound semiconductor alloy systems that an anticrossing interaction within the valence band will influence the optical properties of the group IV alloy  $\text{Sn}_x\text{Ge}_{1-x}$  as well.

The composition dependence of the direct band gap ( $E_g$ ) and spin-orbit splitting ( $\Delta_0$ ) energies of  $\text{Sn}_x\text{Ge}_{1-x}$  thin films with Sn concentrations up to  $x=0.064$  was investigated with photomodulated reflectance (PR) spectroscopy. The films were grown on Ge (001) substrates by molecular beam epitaxy (MBE) in a Riber EVA 32 Si MBE system. A Ge buffer layer approximately 100 nm in thickness was first deposited at 450 °C followed by Sn-Ge codeposition at 150 °C. The resulting  $\text{Sn}_x\text{Ge}_{1-x}$  films ranged in thickness from 100 to 200 nm and were fully strained as determined by x-ray diffraction analysis. The final alloy compositions were ascertained by Rutherford backscattering spectrometry, which also verified that the films were of good crystalline quality. Photomodulated reflectance spectroscopy was carried out at room temperature. The probe beam consisted of monochromatic light from a tungsten halogen lamp, and a HeCd laser ( $\lambda=325$  and 442 nm) served as the modulation source. The transition energies were then established by fitting the spectra to the Aspnes third-derivative functional form.<sup>11</sup>

The PR spectra of the  $\text{Sn}_x\text{Ge}_{1-x}$  samples are displayed in Fig. 1. Both the direct band gap ( $E_g$ ) and spin-orbit split-off band to conduction band ( $E_g+\Delta_0$ ) transitions in the  $\text{Sn}_x\text{Ge}_{1-x}$  film decrease in energy with increasing Sn concentration relative to those transitions in the Ge substrate ( $E_g=0.8$  eV and  $E_g+\Delta_0=1.1$  eV). To account for the effects of strain within the film, the experimentally measured band gap and spin-orbit splitting energies were subsequently corrected according to a strained Luttinger Hamiltonian method.<sup>12</sup> The composition dependence of the  $E_g$  and  $\Delta_0$  energies determined by these measurements is consistent with that reported in the literature.<sup>2,3</sup> While the VCA predicts a reduction in  $E_g$  by approximately 12 meV per  $x=0.01$ , the experimentally measured values decrease by about 30 meV per  $x=0.01$ , indicative of the strong bowing phenomenon. The compositional trend in  $\Delta_0$ , on the other hand, closely follows the VCA predictions with a modest increase of approximately 5 meV per  $x=0.01$ .

The key for understanding the physical mechanisms behind the bowing trends in the direct optical transitions of  $\text{Sn}_x\text{Ge}_{1-x}$  lies in the evaluation of the mismatch in electronegativities and ionization energies between the two elements.

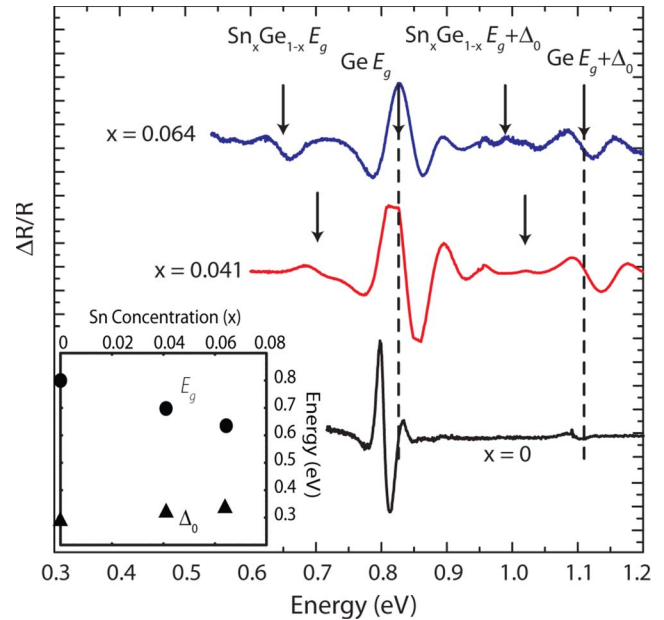


FIG. 1. (Color online) Room temperature PR spectra of  $\text{Sn}_x\text{Ge}_{1-x}$  ( $0 < x < 0.064$ ). The inset displays the uncorrected transition direct band gap and spin-orbit splitting energies.

Unlike  $\text{Si}_x\text{Ge}_{1-x}$ , in which the mismatch between Si and Ge is slight and the alloy exhibits very little bowing behavior, Sn has a much lower electronegativity and ionization energy (1.7 and 7.2 eV, respectively) than Ge (1.8 and 7.9 eV), leading to the localization of holes at the  $p$ -like states of the Sn impurity atoms.<sup>13</sup> The VBAC model captures the effects that this localization has on the electronic band structure of the alloy by considering the interaction between localized  $T_2$  symmetric states of the Sn impurities and the valence band of the Ge host in addition to the linear shift in the band edges predicted by the VCA. A simplified picture of the  $\text{Sn}_x\text{Ge}_{1-x}$  valence band at the  $\Gamma$  point may be derived within the  $k \cdot p$  formalism using a  $12 \times 12$  Hamiltonian matrix, which is composed from the two identical basis sets of six time-reversal symmetry-invariant wave functions that make up the Ge valence band and Sn states. The exact form of the model and details of the calculations can be found in a previous report on its application to III-V alloys.<sup>7</sup>

In order to account for the indirect to direct gap crossover at  $x=0.1$ , the conduction band bowing parameter at the  $\Gamma$  point was set to  $b_{CB-\Gamma}=0.70$  eV, while that of the  $L$  point was assumed to be negligible, as previously discussed by D'Costa *et al.*<sup>3</sup> The bowing of the valence band edge was then treated by the VBAC model. The strength of the anticrossing behavior is determined by both the mismatch in ionization energy between Ge and Sn and the proximity of the interacting states. The qualitative effect of the mismatch is represented in the hybridization energy through an empirically determined coupling parameter  $C_{\text{Sn}}$ . In this case, the position of the primary  $p$ -like defect states of Sn ( $E_{\text{Sn}}$ ) must also be used as a fitting parameter, as it has not been ascertained experimentally.

The best fit of the VBAC model to the direct optical transitions measured by PR was obtained with a coupling parameter of  $C_{\text{Sn}}=1.4$  eV and a Sn defect position at  $E_{\text{Sn}}=$

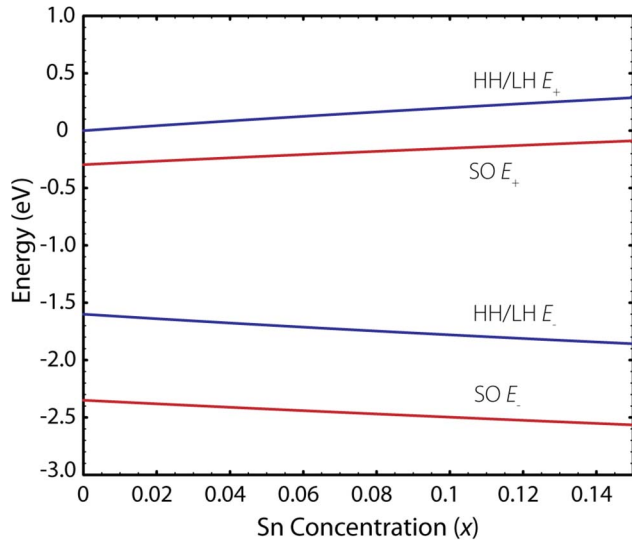


FIG. 2. (Color online) Positions of the  $\text{Sn}_x\text{Ge}_{1-x}$  valence subbands at the  $\Gamma$  point relative to the VBM of Ge as a function of alloy composition.

$-1.6$  eV relative to the VBM of Ge. Using a spin-orbit splitting energy of  $0.8$  eV for the Sn valence  $p$  states, the spin-orbit split-off position  $E_{\text{Sn } SO}$  is located at  $-2.4$  eV.<sup>14</sup> Although much more modest, these parameters fall within the range of those used to describe other HMAs.<sup>7-10</sup> Figure 2 illustrates the positions of the restructured valence subband at  $k=0$  as a function of Sn concentration. At the  $\Gamma$  point, only the wave functions of identical symmetry will couple, leading to a series of two-level anticrossing interactions between the heavy hole (HH), light hole (LH), and spin-orbit split-off (SO) states of Sn and Ge, respectively. Each interaction subsequently produces a set of  $E_+$  and  $E_-$  subbands that are of mixed character and diverge in energy. In  $\text{Sn}_x\text{Ge}_{1-x}$ , the  $E_+$  subbands derive from the Ge valence band and are predominantly extended in nature, while the  $E_-$  subbands originate from the Sn states and remain largely localized.

From the framework of the VBAC model, it is evident that the interaction between the Sn and Ge states produces a much more substantial degree of bowing in the valence band edge than previously predicted by the quadratic bowing relationship and is a significant source of the large bowing in the direct band gap of  $\text{Sn}_x\text{Ge}_{1-x}$ . Likewise, the interaction of the spin-orbit split-off states produces a comparable upward movement of the SO  $E_+$  subband such that there is very little bowing of the spin-orbit splitting energy. These predictions are in good agreement with the strain-corrected direct band gap and spin-orbit splitting energies that were measured for this study as well as those values reported in the literature, shown in Fig. 3.<sup>2,3</sup> The final composition dependence of the conduction and valence band edges calculated in this study is displayed in Fig. 4 along with the trends predicted by the VCA and quadratic bowing relationships for comparison.

In its present form, the VBAC model is limited to the analysis of the valence band restructuring in this low band gap alloy specifically at the  $\Gamma$  point. If expanded to include the additional interaction between the valence band and conduction band states, however, this model may be used to

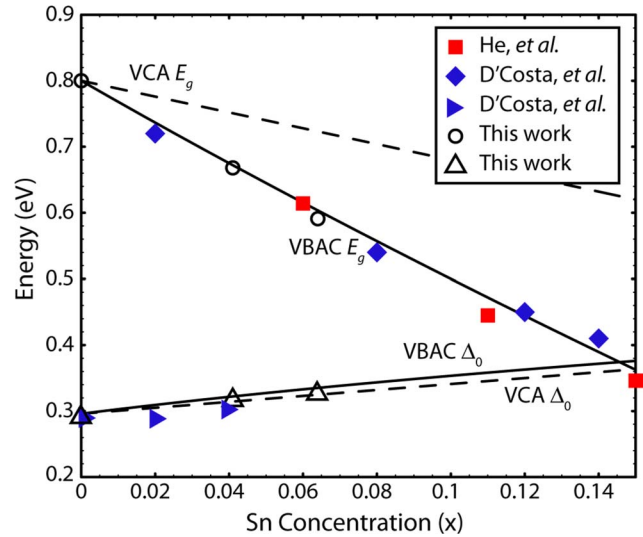


FIG. 3. (Color online) Compositional dependencies of the direct band gap ( $E_g$ ) and spin-orbit splitting ( $\Delta_0$ ) energies of  $\text{Sn}_x\text{Ge}_{1-x}$  (Refs. 2 and 3). The solid and dashed lines represent the VBAC and VCA-predicted trends, respectively.

calculate the band structure around the  $\Gamma$  point. Because the Sn defect levels are resonant with the Ge valence band, the anticrossing interactions will not only push the  $E_+$  subbands upward in energy, but they will also cause the bands to flatten in  $k$  space and result in an increase in the hole effective masses. Considering alloy disorder scattering to be the dominant scattering mechanism in low and moderately doped unstrained  $\text{Sn}_x\text{Ge}_{1-x}$  films, the hole mobility should actually decrease with an increase in Sn concentration. The actual effect of alloying on the electron and hole mobilities, though, remains to be investigated.

Most importantly, the extension of the band anticrossing

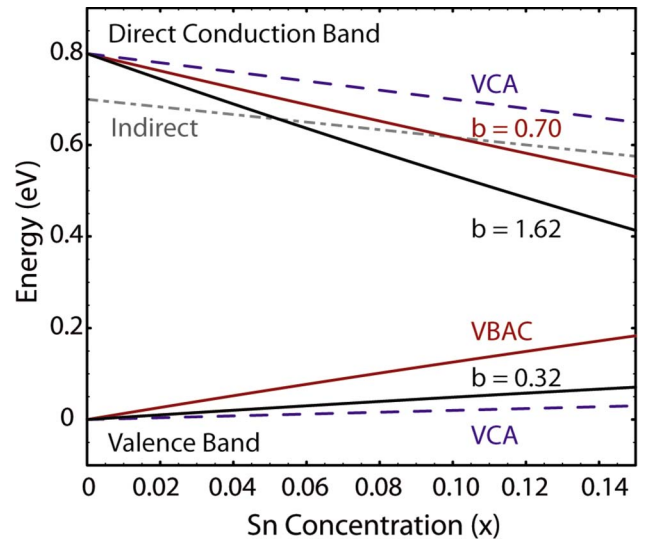


FIG. 4. (Color online) Bowing of the conduction and valence bands predicted by the VBAC model ( $b=0.7$  eV and VBAC), the VCA (dashed lines), and the quadratic bowing relationship ( $b=1.62$  and  $0.32$  eV). The composition dependence of the indirect  $E_g$  is also shown (dashed-dotted line).

concept to  $\text{Sn}_x\text{Ge}_{1-x}$  opens the possibility of understanding, predicting, and engineering the optical properties of other highly mismatched IV-IV alloys in a similar manner. From the analysis of the VBAC interactions presented here, the binary alloy  $\text{Sn}_x\text{Si}_{1-x}$  is expected to exhibit an even greater degree of band gap bowing than that observed in  $\text{Sn}_x\text{Ge}_{1-x}$  due to the large mismatch in electronegativity between Si and Sn and increased proximity between the coupled states. Assuming a VBM offset of  $-0.3$  eV between Si and Ge, the Sn states are located at  $E_{\text{Sn}} = -1.3$  eV and  $E_{\text{Sn } SO} = -2.1$  eV in Si. Band anticrossing could also occur within the conduction bands of  $\text{Si}_{1-x}\text{C}_x$  and  $\text{Ge}_{1-x}\text{C}_x$ . From the anticrossing behavior observed in III-V and II-VI HMAs, the highly electronegative nature of C is predicted to localize electrons at the  $A_1$  symmetric states of the impurity atoms and leads to a restructuring of the conduction band in much the same manner as has been demonstrated in compound semiconductor HMAs.<sup>7,9,15</sup> This approach, in particular, may also be effective in yielding a direct gap IV-IV alloy given that the anticrossing behavior has been shown to be most prominent at the  $\Gamma$  point and has induced an indirect to direct transition in  $\text{GaN}_x\text{P}_{1-x}$ .<sup>15</sup>

In summary, the large bowing of the direct band gap of  $\text{Sn}_x\text{Ge}_{1-x}$  has been shown in part to be the product of a con-

siderable bowing of the valence band edge. Restructuring of the valence band into  $E_+$  and  $E_-$  subbands, which occurs via an anticrossing interaction between the localized  $p$ -like states of the Sn impurity atoms and the extended  $p$ -like states of the Ge host, leads to a strong upward shift in the valence band edge but does not significantly affect the spin-orbit splitting energy. The anticrossing phenomenon not only provides a fundamental explanation for the large bowing behavior in the optical transitions of  $\text{Sn}_x\text{Ge}_{1-x}$ , but it could ultimately be used to understand the band structure and electronic transport properties of this and other IV-IV HMA systems.

This research was carried out at the Jet Propulsion Laboratory, California Institute of Technology, under a contract with the National Aeronautics and Space Administration and funded through the internal Research and Technology Development program. This work is also supported by the Director, Office of Science, Office of Basic Energy Sciences, Division of Materials Sciences and Engineering, of the U.S. Department of Energy under Contract No. DE-AC02-05CH11231. K.A. acknowledges support from an NSF-IGERT traineeship.

<sup>1</sup>A. Harwit, P. R. Pukite, J. Angilello, and S. S. Iyer, *Thin Solid Films* **184**, 395 (1990).

<sup>2</sup>G. He and H. A. Atwater, *Phys. Rev. Lett.* **79**, 1937 (1997).

<sup>3</sup>V. R. D'Costa, C. S. Cook, A. G. Birdwell, C. L. Littler, M. Canonico, S. Zollner, J. Kouvetakis, and J. Menendez, *Phys. Rev. B* **73**, 125207 (2006).

<sup>4</sup>R. A. Soref and C. H. Perry, *J. Appl. Phys.* **69**, 539 (1991).

<sup>5</sup>J. D. Sau and M. L. Cohen, *Phys. Rev. B* **75**, 045208 (2007).

<sup>6</sup>R. S. Bauer and G. Margaritondo, *Phys. Today* **40** (1), 27 (1987).

<sup>7</sup>W. Shan, K. M. Yu, W. Walukiewicz, J. W. Ager III, E. E. Haller, and M. C. Ridgway, *Appl. Phys. Lett.* **75**, 1410 (1999).

<sup>8</sup>K. Alberi, J. Wu, W. Walukiewicz, K. M. Yu, O. D. Dubon, S. P. Watkins, C. X. Wang, X. Liu, Y.-J. Cho, and J. Furdyna, *Phys. Rev. B* **75**, 045203 (2007).

<sup>9</sup>K. M. Yu, W. Walukiewicz, J. Wu, W. Shan, J. W. Beeman, M. A. Scarpulla, O. D. Dubon, and P. Becla, *Phys. Rev. Lett.* **91**, 246403 (2003).

<sup>10</sup>J. Wu, W. Walukiewicz, K. M. Yu, J. W. Ager, E. E. Haller, I. Miotkowski, A. K. Ramdas, C. H. Su, I. K. Sou, R. C. C. Perera, and J. D. Denlinger, *Phys. Rev. B* **67**, 035207 (2003).

<sup>11</sup>D. E. Aspnes, *Surf. Sci.* **37**, 418 (1973).

<sup>12</sup>R. People and S. K. Sputz, *Phys. Rev. B* **41**, 8431 (1990).

<sup>13</sup>W. Gordy and W. J. O. Thomas, *J. Chem. Phys.* **24**, 439 (1956).

<sup>14</sup>D. J. Chadi, *Phys. Rev. B* **16**, 790 (1977).

<sup>15</sup>J. Wu, W. Walukiewicz, K. M. Yu, J. W. Ager, E. E. Haller, Y. G. Hong, H. P. Xin, and C. W. Tu, *Phys. Rev. B* **65**, 241303(R) (2002).